COMPREHENSIVE ACTIVE MICROVIBRATION CONTROL SYSTEM USING PIEZOELECTRIC ACTUATORS FOR BASE-ISOLATED PRECISION MANUFACTURING FACILITIES

Mamoru SHIMAZAKI[1], Takafumi FUJITA[2], Yoshiyuki HASHIMOTO[3], Hirokazu YOSHIOKA[3], Takashi KITAHARA[4] and Tomohiro OGAWA[5]

ABSTRACT: In order to achieve more perfect vibration-free environment in base-isolated precision manufacturing facilities, a smart structure was tested for comprehensive active microvibration control in a base-isolated 2-story steel frame building model of a $5\times3\times4^{H}$ m external size and a 6,900 kg total mass. In the building model, 20 piezoelectric actuators were attached to the columns and the beams, and four horizontal actuator units consisting of two piezoelectric actuators each and four vertical ones of the same type were installed between the bottom of the superstructure and the foundation. The tests showed that the smart structure could effectively control three-dimensional microvibrations generated in the building model and excited by external disturbances.

Key Words: Microvibration, Precision Manufacturing Facility, Active Control, Smart Structure, Piezoelectric Actuator, Base-Isolation, Model Matching Method, Modal Analysis, FEM

INTRODUCTION

It is expected that the active microvibration control will be applied to floors and even entire buildings to meet requirements for more perfect vibration-free environment in precision manufacturing facilities [1]. Furthermore, particularly in Japan, it is desirable that such facilities are effectively protected from earthquake attacks by seismic isolation. Therefore, comprehensive active microvibration system will be required in such base-isolated precision manufacturing facilities, in order to control both microvibrations generated by equipments and people in the buildings and excited by external disturbances such as ambient ground vibrations and winds. In this study, a smart structure was tested for comprehensive active microvibration control in a base-isolated 2-story steel frame building model which was supported by four multistage rubber bearings. In the building model, 20 piezoelectric actuators were attached to the columns and the beams, and four horizontal actuator units consisting of two piezoelectric actuators each and four vertical ones of the same type were installed between the bottom of the superstructure and the foundation.

[1] Technical Associate, Institute of Industrial Science, The University of Tokyo
[2] Professor, Institute of Industrial Science, The University of Tokyo
[3] Takenaka Corporation
[4] Hitachi Plant Engineering & Construction Co., Ltd.
[5] Sumitomo Heavy Industries, Ltd.

EXPERIMENTAL MODEL

Figure 1 shows a photograph of the building model used in the study. The building model was a base-isolated 2-story steel frame structure of a $5\times3\times4^{H}$ m external size and a 6,900 kg total mass which was supported by four multistage rubber bearings. Two shakers were installed in the center of the first floor to simulate the three-dimensional microvibrations generated by equipments and people in the buildings.

Each column of the first story had a stage in its bottom part, and four piezoelectric actuators of a $25\times25\times36^{H}$ mm external size were installed in each stage to control the bending moment of the column in the two lateral directions (Figure 2). Each beam of the second floor in the longitudinal direction had a stage at its midpoint, and two piezoelectric actuators of the same size were installed in each stage to control the bending moment of the beam in the vertical direction. (Figure 3)

Figure 4 shows a method for controlling the bending moment via piezoelectric actuators. Exactly before the control starts, the actuators on both sides of the column/beam are slightly lengthened by a bias input voltage. This state becomes the equilibrium state during the control. Then the actuators are lengthened or shortened with respect to the equilibrium state by a control voltage. Therefore, the actuators can push and pull the arms attached to the column/beam and can control the bending moments applied to the column/beam as shown in Fig. 4 [2].

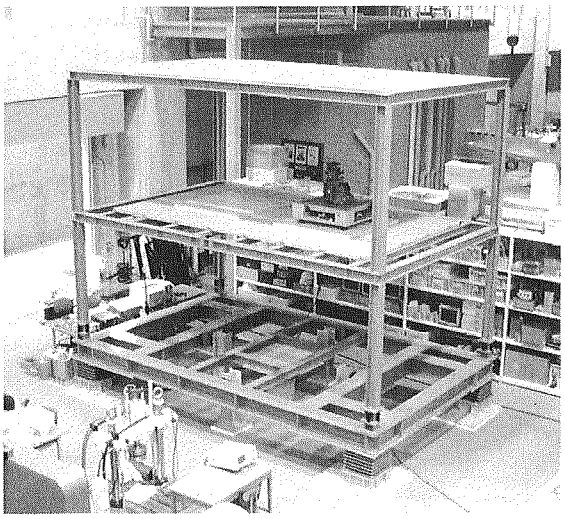

Figure 1 Building model

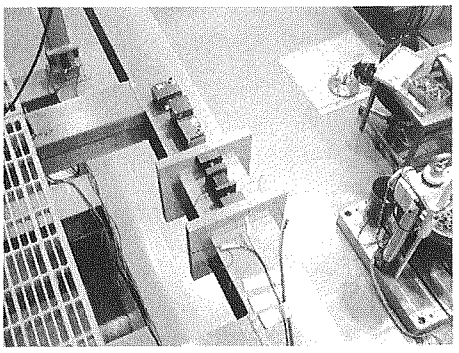

Figure 3 Piezoelectric actuators attached to beam

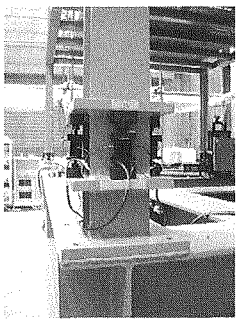

Figure 2 Piezoelectric actuators attached to column

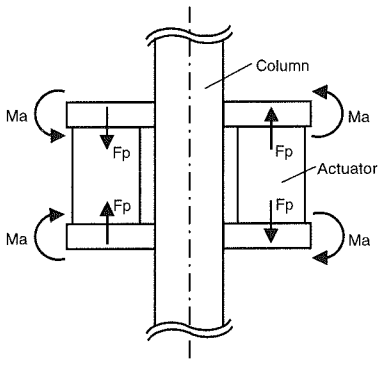

Figure 4 Installation method of actuator in stage

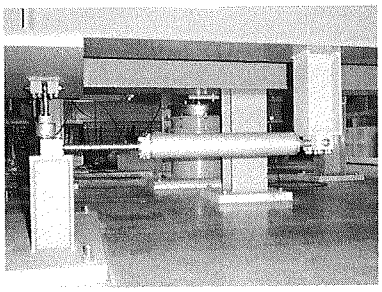

Figure 5 Horizontal actuator unit

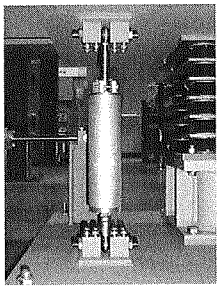

Figure 6 Vertical actuator unit

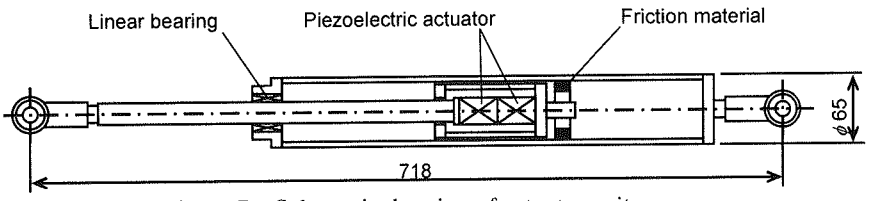

Figure 7 Schematic drawing of actuator unit

As shown in Figs. 5 and 6, four horizontal actuator units consisting of two piezoelectric actuators each and four vertical ones of the same type were installed between the bottom of the superstructure and the foundation. Figure 7 shows a schematic drawing of the actuator unit. The actuator units slide to protect the piezoelectric actuators when an earthquake occurs.

ANALYTICAL MODEL

The FEM analysis was carried out for the building model to obtain its natural frequencies, mode shapes, and participation factors. Figure 8 shows ten modes that were selected as the control objects. They were the first, fourth, and eighth modes in which deformations of the columns in the transverse (short side) direction were dominant, the second, sixth and tenth modes in which deformations of the columns in the longitudinal (long side) direction were dominant, the fifth and seventh mode in which the two beams in the longitudinal direction of the second or roof floor vibrated in the same vertical directions, the fourteenth mode in which the beams vibrated in the opposite vertical direction and the sixteenth mode in which the vertical stiffness of rubber bearings mainly governed. In this study, the longitudinal, transverse and vertical directions were the x-direction, the y-direction and the z-direction respectively.

Equations of motion based on the FEM analysis of the building model are written as follows:

$$[M]\{\ddot{X}\}+[K]\{X\}=-[M][H_Z]\{\ddot{Z}\}+[H_F]\{F\}+[H_U]\{U\}+[H_V]\{V\} \tag{1}$$

where

$[M]$: Mass matrix
$[K]$: Stiffness matrix
$[H_z]$: Coefficient matrix for the vector $\{\ddot{Z}\}$
$[H_F]$: Coefficient matrix for the vector $\{F\}$
$[H_U]$: Coefficient matrix for the vector $\{U\}$
$[H_V]$: Coefficient matrix for the vector $\{V\}$

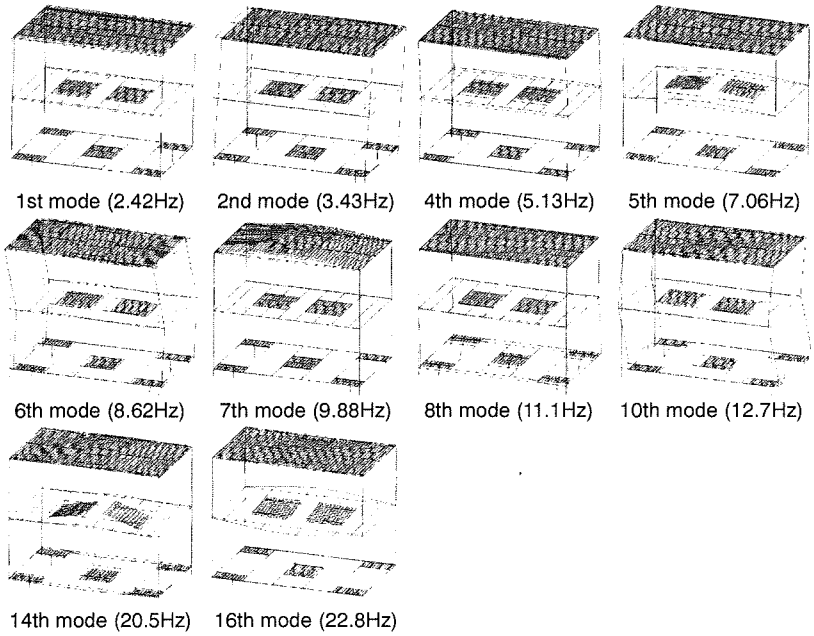

Figure 8 Mode shapes of control objects

$\{X\}=\{x \quad y \quad z \quad \theta_x \quad \theta_y \quad \theta_z\}^T$: Vector of displacements and angles of rotation of the elements

$\{\ddot{Z}\}=\{\ddot{z}_x \quad \ddot{z}_y \quad \ddot{z}_z\}^T$: Vector of the ground accelerations

$\{F\}=\{f_x \quad f_y \quad f_z\}^T$: Vector of the excitation forces of the shakers installed in the center of the first floor

$\{U\}=\{u_x \quad u_y \quad u_{z1} \quad u_{z2}\}^T$: Vector of the control voltages to the actuators attached to the columns and the beams

$\{V\}=\{v_1 \quad v_2 \quad \cdots \quad v_8\}^T$: Vector of the control voltages to the actuator units installed in the seismic isolation layer

The vector $\{X\}$ is expressed by

$$\{X\}=[\phi]\{q\} \tag{2}$$

where $[\phi]$ and $\{q\}$ are the modal matrix and the vector of the modal displacements respectively. The modal matrix is normalized by

$$[\phi]^T[M][\phi]=[I] \tag{3}$$

Considering the modal damping, the modal equation of motion of the i-th mode is obtained as

$$\ddot{q}_i + 2\zeta_i\omega_i\dot{q}_i + \omega_i^2 q_i = -\{B_{Zi}\}\{\ddot{Z}\} + \{B_{Fi}\}\{F\} + \{B_{Ui}\}\{U\} + \{B_{Vi}\}\{V\} \tag{4}$$

where

ξ_i: Modal damping ratio
ω_i: Natural frequency
$\{B_{Zi}\}$: Vector of the participation factors concerning the vector $\{\ddot{Z}\}$
$\{B_{Fi}\}$: Vector of the participation factors concerning the vector $\{F\}$
$\{B_{Ui}\}$: Vector of the participation factors concerning the vector $\{U\}$
$\{B_{Vi}\}$: Vector of the participation factors concerning the vector $\{V\}$

IDENTIFICATION OF MODAL PARAMETERS

The parameters of the analytical model were identified so as to obtain analytical results that are in good agreement with the experimental results in the following transfer functions in each direction.

(*a*) From the ground acceleration to the response accelerations of each floor
(*b*) From the excitation force of the shaker to the response accelerations of each floor
(*c*) From the control voltages to the actuators attached to the columns and the beams to the response accelerations of each floor
(*d*) From the control voltages to the actuator units installed in the seismic isolation layer to the response accelerations of each floor

Excitation forces and the control voltages were generated from random noise in the frequency range of 1 to 50 Hz. Table 1 shows the results of the identification of natural frequencies and damping ratios.

Table 1 Natural frequencies and damping ratios

Mode	Natural frequency [Hz]		Damping ratio [%]
	Exp.	Cal.	Cal.
1st	2.50	2.42	1.3
2nd	3.48	3.43	1.3
4th	5.42	5.13	1.1
5th	7.54	7.06	0.5
6th	8.72	8.62	2.5
7th	9.82	9.88	1.0
8th	10.7	11.1	5.0
10th	12.4	12.7	5.0
14th	18.4	20.5	0.3
16th	23.3	22.8	1.0

DESIGN OF CONTROLLERS

The controllers for the smart structure were designed by a model-matching method to control the nine modes [3]. Figure 9 shows a block diagram of the general control system, where u, y, v and d represent the control input, output, observation noise and disturbance respectively. From the block diagram, y is expressed as

$$y = P_{dy}d + P_{uy}u \tag{5}$$

where P_{dy} and P_{uy} are the open loop transfer functions of the plant from d to y, and from u to y,

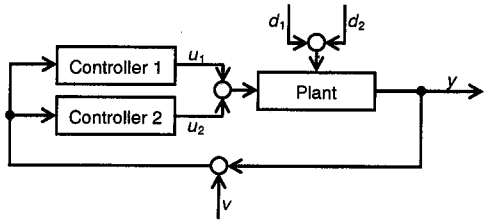

Figure 9 Block diagram of general control system

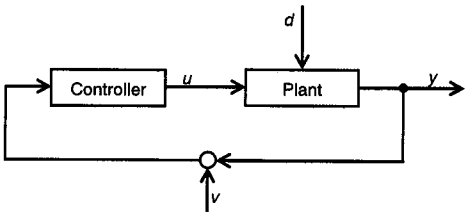

Figure 10 Block diagram of control system in this study

respectively. Since $u = C_{ru} r + C_{yu}(y + v)$, Eq. (5) is transformed to

$$y = (1 - P_{uy} C_{yu})^{-1} (P_{uy} C_{ru} r + P_{uy} C_{yu} v + P_{dy} d) \tag{6}$$

where C_{ru} and C_{yu} are the open loop transfer functions of the controller from r to u, and from y to u, respectively. Three closed loop transfer functions are defined by the following equations:

$$W_{ry} = (1 - P_{uy} C_{yu})^{-1} P_{uy} C_{ru} \tag{7}$$

$$W_{vy} = (1 - P_{uy} C_{yu})^{-1} P_{uy} C_{yu} \tag{8}$$

$$W_{dy} = (1 - P_{uy} C_{yu})^{-1} P_{dy} \tag{9}$$

where W_{ry}, W_{vy} and W_{dy} are the closed loop transfer functions from r to y, from v to y, and from d to y, respectively. From Eqs. (7), (8) and (9),

$$W_{dy} = (1 + W_{vy}) P_{dy} \tag{10}$$

$$C_{yu} = P_{uy}^{-1} W_{vy} (1 + W_{vy})^{-1} \tag{11}$$

are obtained, where P_{dy} and P_{uy} are given. Therefore these equations mean that C_{yu} is uniquely determined by W_{vy} or W_{dy}.

The closed loop transfer function W_{vy} or W_{dy} is determined considering the following conditions:

(1) The transfer functions W_{vy} and W_{ry} must have larger relative orders than P_{uy}.
(2) The sets of zeros of W_{vy} and W_{ry} must contain all zeros of P_{uy}.
(3) The set of zeros of $(1 + W_{ry})$ must contain all poles of P_{uy}.

These three conditions are conditions to obtain a proper controller.

Figure 10 shows a block diagram of the control system in this study, where u_1 and u_2 are the modal control inputs, d_1 and d_2 the modal disturbances, y is the modal output and v the observation noise. From the block diagram, y is expressed as

$$y = P_{d_1 y} d_1 + P_{d_2 y} d_2 + P_{u_1 y} u_1 + P_{u_2 y} u_2 \tag{12}$$

In the control system, two modal control voltages were input to the plant (u_1 is the modal control voltage for the actuators attached to the columns and the beams and u_2 is for the actuator units installed in the seismic isolation layer), and two modal disturbances were input to the plant (d_1 by the shakers and d_2 by ambient ground vibration). The controllers were designed independently. W_{d1y} and W_{d2y} were chosen as follows:

$$W_{d_1 y} = \frac{s^2(s^4 + \gamma_3 s^3 + \gamma_2 s^2 + \gamma_1 s + \gamma_0)}{(s - p_1)(s - p_2)\cdots(s - p_6)} \tag{13}$$

$$W_{d_2 y} = \frac{(2\zeta_i \omega_i s + \omega_i^2)(s^5 + \gamma_4 s^4 + \gamma_3 s^3 + \gamma_2 s^2 + \gamma_1 s + \gamma_0)}{(s - p_1)(s - p_2)\cdots(s - p_7)} \tag{14}$$

Then, the controller transfer functions C_{yu1} and C_{yu2} were calculated by

$$C_{yu_1} = P_{u_1 y}^{-1} W_{vy}\left(1 + W_{vy}\right)^{-1} = \frac{\beta_1 s^2 + \beta_0 s}{s^4 + \gamma_3 s^3 + \gamma_2 s^2 + \gamma_1 s + \gamma_0} \tag{15}$$

$$C_{yu_2} = P_{u_2 y}^{-1} W_{vy}\left(1 + W_{vy}\right)^{-1} = \frac{\beta_2 s^3 + \beta_1 s^2 + \beta_0 s}{s^5 + \gamma_4 s^4 + \gamma_3 s^3 + \gamma_2 s^2 + \gamma_1 s + \gamma_0} \tag{16}$$

MICROVIBRATION CONTROL PERFORMANCES

The tests were carried out in cases when controlled with the actuators attached to the columns and beams, controlled with the actuator units installed in the seismic isolation layer and controlled with all the actuators. Figure 11 compares transfer functions from the ground acceleration to the response accelerations on the 1st floor, 2nd floor, and the roof floor in each direction. In each case, effective reductions were obtained in each mode, which were selected as the control objects. Figure 12 compares transfer functions from the excitation force of the shaker to the response accelerations on the 1st floor, 2nd floor, and the roof floor in each direction. In each case, effective reductions were obtained in each mode, which were selected as the control objects.

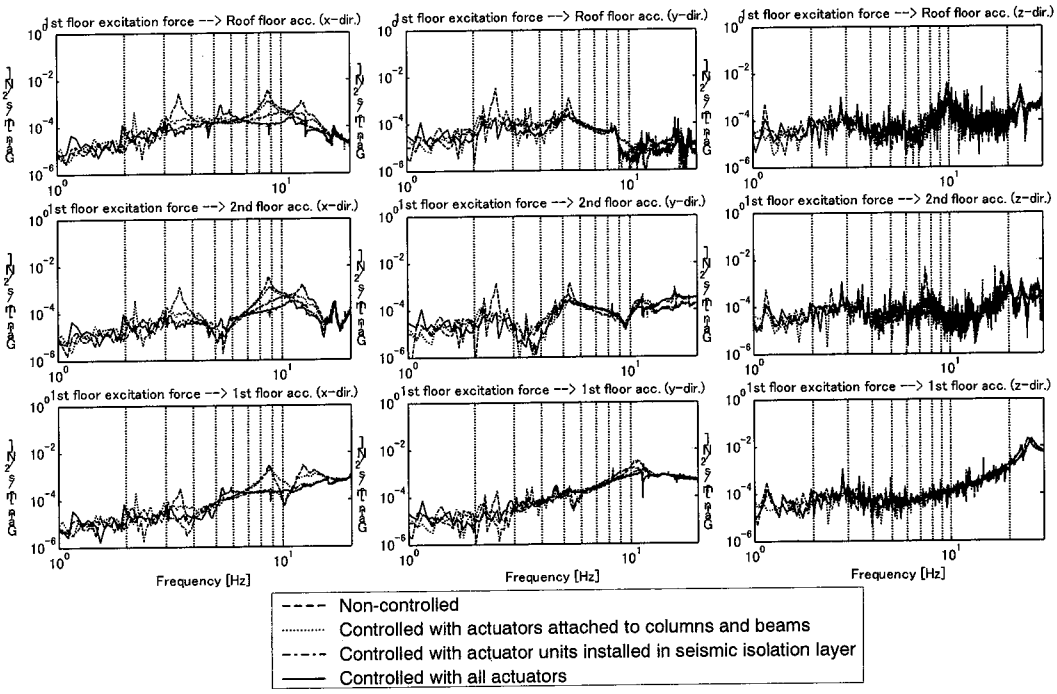

Figure 11 Transfer functions from ground acceleration to response accelerations

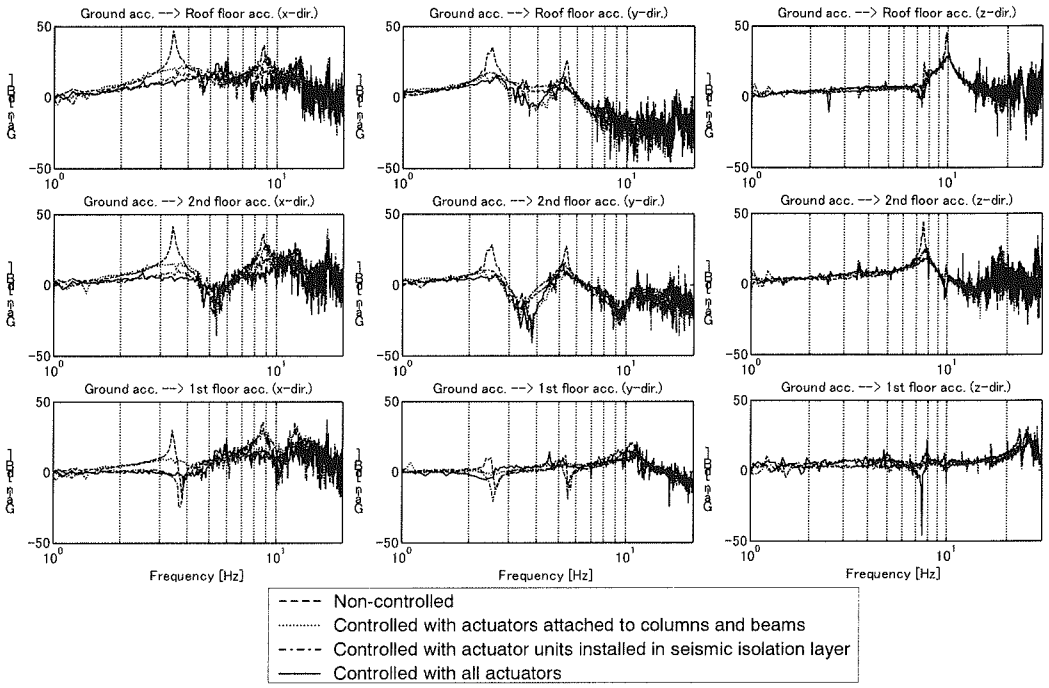

Figure 12 Transfer functions from excitation force to response accelerations

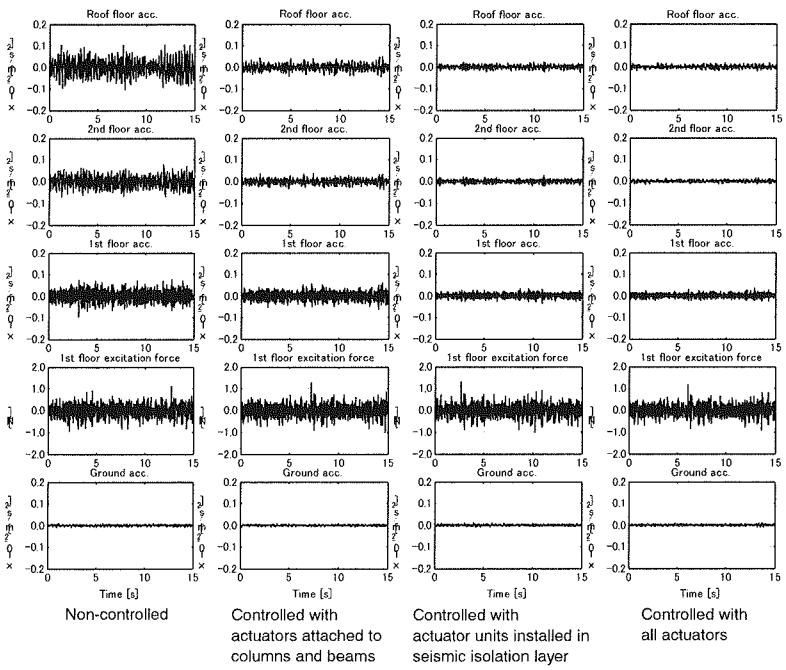

Figure 13 Time histories (x-direction)

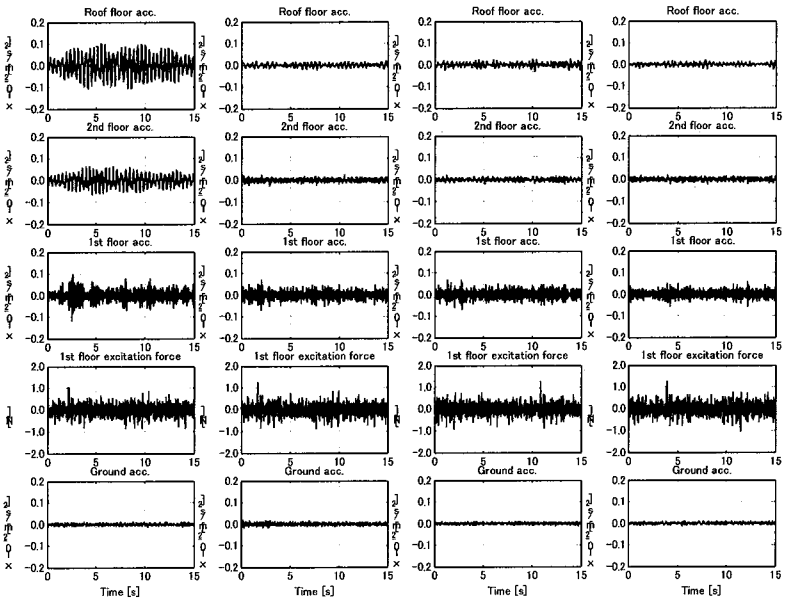

Figure 14 Time histories (y-direction)

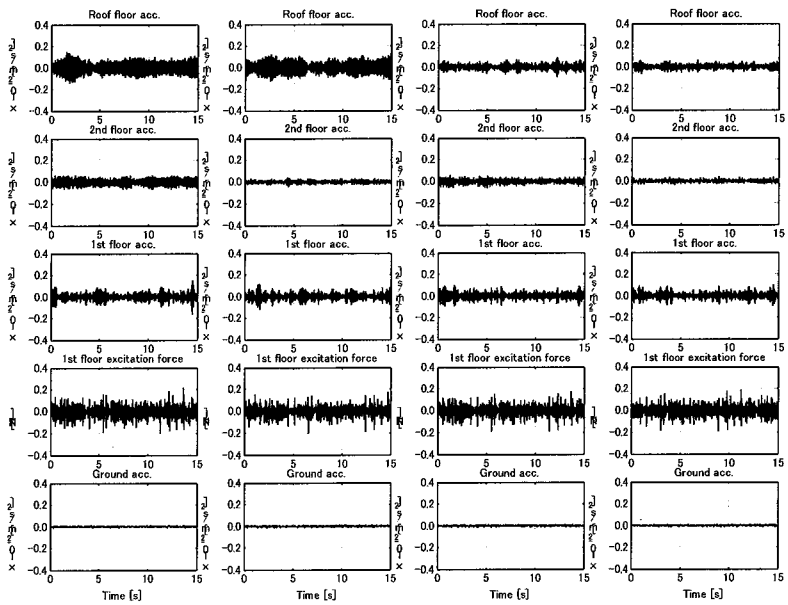

Figure 15 Time histories (z-direction)

Figs. 13, 14 and 15 compares time histories in each direction obtained by the tests, including the ground accelerations, excitation forces of the shaker installed in the 1st floor, the 1st floor accelerations, the 2nd floor accelerations and the roof accelerations. The maximum amplitudes of the control voltages were about ± 2 V, whereas the capacity of the actuators was ± 50 V, showing that the capacity of the actuators had a large margin. Figure 16 shows the rms values of the 1st floor, 2nd floor, and the roof floor accelerations. The response accelerations were reduced in the rms values of those when non-controlled. Especially, in the case where controlled with all actuators was effective.

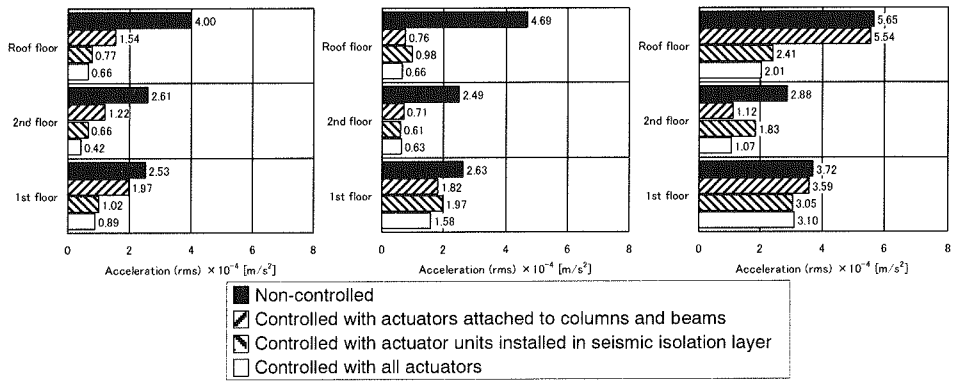

Figure 16. Rms values of response accelerations

CONCLUSIONS

In this study, the smart structure for the comprehensive active microvibration control of base-isolated precision manufacturing facilities was tested using the 2-story steel frame building model in which the piezoelectric actuators attached to the columns and the beams for the bending moment control of them, and four horizontal actuator units consisting of two piezoelectric actuators each and four vertical ones of the same type were installed between the bottom of the superstructure and the foundation. Through the tests, it was demonstrated that the smart structure using piezoelectric actuators had a large feasibility for the comprehensive active microvibration control of the base-isolated building. Furthermore, it was confirmed that the comprehensive active microvibration control for base-isolated structures using actuators attached to the columns/beams and actuator units installed in the seismic isolation layer was effective.

REFERENCES

1. T. Fujita, "Smart Structures for Active Vibration Control of Buildings," Proc. of the 1997 International Symposium on Active Control of Sound and Vibration (ACTIVE 97), pp. XIX-XXXIII, Budapest, Hungary, 1997
2. T. Kamada, T. Fujita, T. Hatayama, T. Arikabe, N. Murai, S. Aizawa, and K. Tohyama, "Active vibration control of frame structures with smart structures using piezoelectric actuators (Vibration control by control of bending moments of columns)," Smart Materials and Structures, Vol. 6, No. 4, pp. 448-456, 1997
3. T. Fujita, Y. Tagawa, N. Murai, S. Shibuya, A. Takeshita and Y. Takahashi, "Study of Active Microvibration Control Device Using Piezoelectric Actuator (1st Report, Fundamental Study of One-Dimensional Microvibration Control)," Transactions of the Japan society of mechanical engineers, Vol. 57, No. 540, pp. 2560-2565, 1991 (in Japanese)